

Polymer Photovoltaic Cells: Enhanced Efficiencies via a Network of Internal Donor-Acceptor Heterojunctions

G. Yu,* J. Gao, J. C. Hummelen, F. Wudl, A. J. Heeger

The carrier collection efficiency (η_c) and energy conversion efficiency (η_e) of polymer photovoltaic cells were improved by blending of the semiconducting polymer with C_{60} or its functionalized derivatives. Composite films of poly(2-methoxy-5-(2'-ethyl-hexyloxy)-1,4-phenylene vinylene) (MEH-PPV) and fullerenes exhibit η_c of about 29 percent of electrons per photon and η_e of about 2.9 percent, efficiencies that are better by more than two orders of magnitude than those that have been achieved with devices made with pure MEH-PPV. The efficient charge separation results from photoinduced electron transfer from the MEH-PPV (as donor) to C_{60} (as acceptor); the high collection efficiency results from a bicontinuous network of internal donor-acceptor heterojunctions.

The need to develop inexpensive renewable energy sources continues to stimulate new approaches to production of efficient, low-cost photovoltaic devices. Although inorganic semiconductors (silicon, amorphous silicon, gallium arsenide, and sulfide salts) have been the primary focus, the photosensitivity and the photovoltaic effects in devices made with organic materials have also been explored, including conjugated polymers (1), organic molecules (2), stacked discotic liquid crystals (3), and self-assembling organic semiconductors (4). Because of the advantages that would be realized with polymer-based photovoltaics (such as low-cost fabrication in large sizes and in desired shapes), efficient "plastic" solar cells would have a major impact.

Energy conversion efficiencies of photovoltaic cells made with pure conjugated polymers were typically 10^{-3} to $10^{-2}\%$, (1), too low to be used in applications. The discovery of photoinduced electron transfer in composites of conducting polymers as donors and buckminsterfullerene (C_{60}) and its derivatives as acceptors (5) provided a molecular approach to high-efficiency photovoltaic conversion (6, 7). Because the time scale for photoinduced charge transfer is subpicosecond, more than 10^3 times faster than the radiative or nonradiative decay of photoexcitations (5), the quantum efficiency of charge separation from donor to acceptor is close to unity. Thus, photoinduced charge transfer across a donor-acceptor (D-A) interface provides an effective way to overcome early time-carrier recombination in organic systems and thus to enhance their optoelectronic response. For example, with the addition of only 1% C_{60} , the photoconductivity increases by an order of magnitude over that of pure MEH-PPV (6, 7).

Although the quantum efficiency for

photoinduced charge separation is near unity for a D-A pair, the conversion efficiency in a bilayer heterojunction device is limited (8). Efficient charge separation occurs only at the D-A interface; thus, photoexcitations created far from the D-A junction recombine before diffusing to the heterojunction. Even if charges are separated at the D-A interface, the conversion efficiency is limited by the carrier collection efficiency.

Consequently, interpenetrating phase-separated D-A network composites (see Fig. 1) would appear to be ideal photovoltaic materials (9-11). Through control of the morphology of the phase separation into an interpenetrating network, one can achieve a large interfacial area within a bulk material. Because any point in the composite is within a few nanometers of a D-A interface, such a composite is a "bulk D-A heterojunction" material. Because of the interfacial potential barrier, as demonstrated by the built-in potential in the bilayer D-A heterojunction diode (8), ultrafast photoinduced charge transfer and charge separation will occur with quantum efficiency approaching unity, leaving holes in the donor phase and electrons in the acceptor phase. This process is illustrated in the upper portion of Fig. 1. If the network is bicontinuous, the collection efficiency can, in principle, be equally efficient.

Such a bicontinuous D-A network material is promising for use in thin-film solar cells. In addition to the high quantum efficiency of charge separation, the electronic structure of such a bicontinuous D-A network allows one to choose contact electrodes with work functions that optimize the carrier collection efficiencies of holes from the donor phase and electrons from the acceptor phase. Thus, thin-film sandwich devices with bicontinuous D-A composites as the active material promise to function as efficient solar cells with high η_c and η_e . Here, we report efficient photovoltaic cells made with such MEH-PPV: C_{60} composites (see Fig. 1).

The device structure consisted of a metal (Ca or Al) contact on the surface of a blend film on a glass (or mylar) substrate, coated with transparent indium-tin-oxide (ITO), as shown in the bottom portion of Fig. 1. The active area of the test devices was 0.1 cm^2 (12). Large photocells ($> 15 \text{ cm}^2$) with similar efficiencies have also been fabricated. MEH-PPV: C_{60} films were spin-cast from 0.3 to 0.5 weight % xylene solutions prepared by mixing of two master solutions in proper ratios. The MEH-PPV (13) was obtained from UNIAX Corporation (Santa Barbara, California) and the C_{60} from MER Corporation (Tucson, Arizona). Typical film thicknesses were 1000 to 2000 Å. The Al or Ca electrode was vacuum evaporated to a thickness between 1000 and 5000 Å.

The limited solubility of pure C_{60} in organic solvents and its tendency to crystallize during film formation limit its use in high-concentration blends. To overcome these problems, a series of soluble C_{60} derivatives has been developed (14). The molecular structures of two C_{60} derivatives, denoted as [6,6]PCBM and [5,6]PCBM, are shown in the top portion of Fig. 1. With these soluble derivatives we have been able to make homogeneous stable blends containing more than 80 weight % fullerene molecules.

Figure 2 compares the current-voltage (*I-V*) characteristics of a Ca/MEH-PPV:

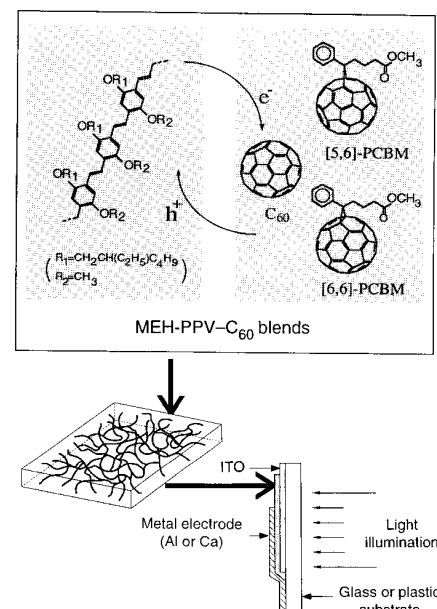


Fig. 1. Schematic diagram of the photoinduced charge transfer process in MEH-PPV: C_{60} D-A blends. The structures of the two soluble C_{60} derivatives used in this study (denoted as [6,6]PCBM and [5,6]PCBM) are included. When cast as a film, the D and A species phase-separate into a bicontinuous network (bulk heterojunction material), as shown schematically. The structure of the photovoltaic cell fabricated with this bulk heterojunction material is sketched at the bottom.

Institute for Polymers and Organic Solids, University of California at Santa Barbara, Santa Barbara, CA 93106-5090, USA.

*Present address: UNIAX Corporation, 6780 Cortona Drive, Santa Barbara, CA 93117-3022, USA.

[6,6]PCBM/ITO device with 1:1 weight ratio (Fig. 2A) and a Ca/MEH-PPV/ITO device (Fig. 2B) in the dark and then illuminated with 20 mW/cm² at 430 nm. For pure MEH-PPV devices, the sharp current turn-on and the open circuit voltage V_{oc} (the minimum in the I - V under photoexcitation) at 1.6 V are consistent with the work-function difference between Ca and ITO.

The similar I - V characteristics of the devices shown in Fig. 2 imply similar device physics. In the Ca/MEH-PPV:[6,6]PCBM/ITO device, the exponential current turn-on shifts to lower voltage by ~ 0.8 V. Thus, the lowest unoccupied molecular orbital of [6,6]PCBM is ~ 0.8 eV below the Fermi energy of Ca. Capacitance measurements of the blend devices yield values similar to those of pure MEH-PPV devices (independent of bias), implying that the energy gap remains clean and trap-free. No indication of ground-state charge transfer was observed.

The forward I - V characteristics of the MEH-PPV devices (Fig. 2B) exhibit three regions: a small shunt current ($< 10^{-10}$ A/cm²) for $V < 1.2$ V, an exponential increase by more than four orders of magnitude between 1.3 and 1.8 V, and "current saturation" at higher voltages (the current increases, but at a less than exponential rate). In reverse bias, the current saturates at approximately 10^{-10} mA/cm² for $|V| < 3$ V. The I - V characteristics at high fields have been interpreted in terms of tunneling (15) into a thin-film semiconductor deplet-

ed of carriers. Capacitance-voltage and alternating current conductivity experiments provide evidence in support of this model (16). The exponential current turn-on and the V_{oc} under strong illumination correspond to the flat band condition.

Because photoinduced electrons in MEH-PPV will lower their energy by transferring to the C_{60} , and photoinduced holes in C_{60} will lower their energy by transferring to the MEH-PPV, the photosensitivity (PS) is substantially enhanced in the phase-separated composite (as shown in Fig. 2). The short-circuit current (I_{sc}) in the MEH-PPV:[6,6]PCBM device is $I_{sc} = 0.5$ mA/cm²; under 20 mW/cm², corresponding to PS = 25 mA/W and $\eta_c = 7.4\%$ electrons per photon (e/ph), both of which are approximately two orders of magnitude higher than those of MEH-PPV devices (Fig. 2B). The electroluminescence quantum efficiency of the blend device was $\sim 3 \times 10^{-7}\%$ photons per electron, 10^3 to 10^4 times less than in pure MEH-PPV devices, which is consistent with ultrafast photoinduced charge separation (5).

The carrier collection and energy conversion efficiencies of the bicontinuous D-A network material are critically dependent on the network's morphology and chemical composition. By changing the solvent from xylene to 1,2-dichlorobenzene we have been able to cast high-quality MEH-PPV:[6,6]PCBM films with methanofullerene compositions up to 1:4 weight

ratio (approximately one acceptor for every polymer repeat unit). For devices made from this blend, $I_{sc} = 2$ mA/cm², PS = 100 mA/W, and $\eta_c \approx 29\%$ e/ph under 20 mW/cm² at 430 nm.

Figure 3 shows η_c (Fig. 3A) and η_e (Fig. 3B) as a function of illumination intensity for several blend devices and for pure MEH-PPV devices. The blend weight ratios are 3:1 for the MEH-PPV: C_{60} device, and 1:1 and 1:4 for the devices using the functionalized fullerenes. For Ca/MEH-PPV:[6,6]PCBM (1:4)/ITO devices, the photosensitivity is slightly sublinear with light intensity ($I^{0.94}$): $\eta_c = 29\%$ e/ph and $\eta_e = 2.9\%$ at 20 mW/cm²; $\eta_c = 45\%$ e/ph and $\eta_e = 3.2\%$ at 10 μ W/cm² (17). In reverse bias, these devices are excellent photodetectors; for example, at -2 V, PS > 200 mA/W and $\eta_c > 60\%$ e/ph at 20 mW/cm², a substantial improvement over earlier results and better than ultraviolet-enhanced silicon photodiodes at 430 nm (7).

The spectral response of these photovoltaic devices is similar to that obtained from photoconductive cells made from MEH-PPV: C_{60} blends (6). The photovoltaic response turns on at approximately 1.5 eV and is relatively flat for photon energy > 2.5 eV.

The PS and the η_c are nearly the same when Al is substituted for Ca as the cathode, although V_{oc} decreases slightly from 0.82 V to 0.68 V at 20 mW/cm². Typical data from Al/MEH-PPV:[6,6]PCBM/ITO devices are also included in Fig. 3. Thus, stable metals with work functions as high as 4.3 eV can be used as the cathode electrode to collect electrons effectively from the acceptor phase.

Ideally, the work function of the anode metal should be close to the donor highest occupied molecular orbital (HOMO) and the work function of the cathode should be close to the acceptor lowest unoccupied molecular orbital (LUMO). An "ohmic" contact would then form selectively at each interface, being ohmic for holes at the interface between the donor and the high-work-function metal contact but blocking for electrons at the same interface, and vice versa. The built-in potential would be the difference between the acceptor LUMO and the donor HOMO.

The bulk D-A heterojunction material provides an automatic selection of electrons from the acceptor component and holes from the donor component. The use of Ca (or Al) as the cathode and ITO as the anode creates a large internal field (for a given film thickness, the internal field is larger with Ca). These two contact materials automatically extract electrons from C_{60} and holes from MEH-PPV. Even though the low-work-function metal is in direct contact with the donor, holes will not be extracted at this interface, because the internal field forces the holes toward the

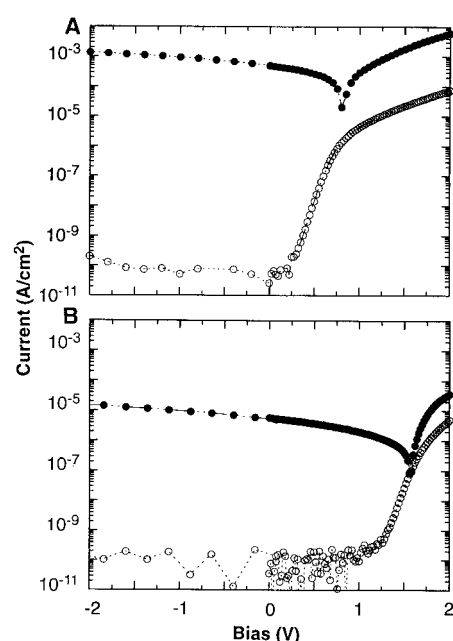


Fig. 2. (A) I - V characteristics of a Ca/MEH-PPV:[6,6]PCBM/ITO device in the dark (open circles) and under 20 mW/cm² of illumination at 430 nm (solid circles). (B) The corresponding data from a Ca/MEH-PPV/ITO device. Currents were plotted as absolute values.

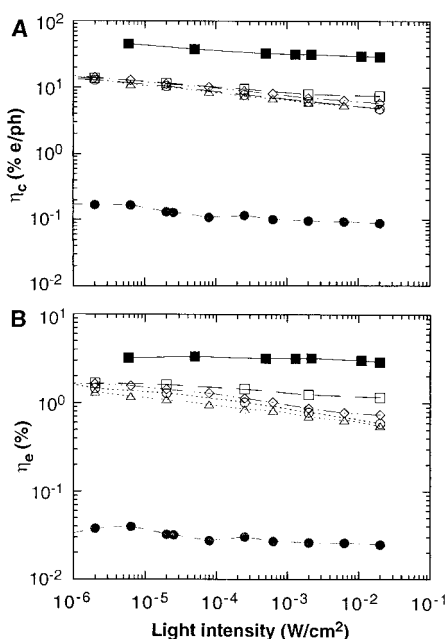


Fig. 3. η_c (A) and η_e (B) of Ca/MEH-PPV:[6,6]PCBM(1:4)/ITO (solid squares); Ca/MEH-PPV:[6,6]PCBM(1:1)/ITO (open squares); Al/MEH-PPV:[6,6]PCBM(1:1)/ITO (diamonds); Ca/MEH-PPV:[5,6]PCBM(1:1)/ITO (open circles); Ca/MEH-PPV: C_{60} (3:1)/ITO (triangles); and Ca/MEH-PPV/ITO (solid circles).

high-work-function contact. For the same reason, electrons are extracted from C₆₀ at the Ca/MEH-PPV:C₆₀ interface. The result, then, is that separated carriers are not "wasted"; they are automatically collected by the proper electrode so that external work can be done.

The substantial enhancement in η_c achieved with the bicontinuous D-A network material results from the large increase in the interfacial area over that in a D-A bilayer and from the relatively short distance from any point in the polymer to a charge-separating interface. Moreover, the internal D-A junctions inhibit carrier recombination and thereby improve the lifetime of the photoinduced carriers (6), so that the separated charge carriers can be efficiently collected by the built-in field from the asymmetric electrodes. Similar effects have been observed in MEH-PPV:Cyano-PPV polymer blends (10, 11).

The device efficiencies are not yet optimized. Because only ~60% of the incident power was absorbed at 430 nm in the thin-film devices used for obtaining the data in Fig. 3, the internal carrier collection efficiency and energy conversion efficiency are approximately 1.7 times larger; that is, $\eta_c \approx 90\%$ e/ph and $\eta_e \approx 5.5\%$ at $10 \mu\text{W}/\text{cm}^2$. Although nearly 100% absorption can be achieved by using thicker films, η_c is currently limited in thick-film devices by internal resistive losses. Further improvements in device efficiencies are expected when the blend composition and the network morphology are optimized.

REFERENCES AND NOTES

1. For a review of photovoltaic devices made with polyacetylene, see J. Kanicki in *Handbook of Conducting Polymers*, T. A. Skotheim, Ed. (Dekker, New York, 1986), pp. 543-660; S. Glenis, G. Tourillon, F. Garnier, *Thin Solid Films* **111**, 93 (1984); S. Karg, W. Riess, V. Dyakonov, M. Schwoerer, *Synth. Metals* **54**, 427 (1993); H. Antoniadis, B. R. Hsieh, M. A. Abkowitz, S. A. Jenekhe, M. Stolk, *ibid.* **64**, 265 (1994); R. N. Marks, J. J. M. Halls, D. D. C. Bradley, R. H. Friend, A. B. Holmes, *J. Phys. Condens. Matter* **6**, 1379 (1994); G. Yu, C. Zhang, A. J. Heeger, *Appl. Phys. Lett.* **64**, 1540 (1994).
2. For an early review, see G. A. Chamberlain, *Solar Cells* **8**, 47 (1983); C. W. Tang, *Appl. Phys. Lett.* **48**, 183 (1986); B. Miller *et al.*, *J. Am. Chem. Soc.* **113**, 6291 (1991); C. H. Lee, G. Yu, D. Moses, A. J. Heeger, *Appl. Phys. Lett.* **65**, 664 (1994).
3. D. Adam *et al.*, *Nature* **371**, 141 (1994).
4. For examples, see B. A. Gregg, M. A. Fox, A. J. Bard, *J. Phys. Chem.* **94**, 1586 (1990); C. Y. Liu, H. L. Pan, H. Tang, M. A. Fox, A. J. Bard, *ibid.* **99**, 7632 (1995).
5. N. S. Sariciftci, L. Smilowitz, A. J. Heeger, F. Wudl, *Science* **258**, 1474 (1992); N. S. Sariciftci and A. J. Heeger, *Intern. J. Mod. Phys. B* **8**, 237 (1994).
6. C. H. Lee *et al.*, *Phys. Rev. B* **48**, 15425 (1993).
7. G. Yu, K. Pakbaz, A. J. Heeger, *Appl. Phys. Lett.* **64**, 3422 (1994).
8. N. S. Sariciftci *et al.*, *ibid.* **62**, 585 (1993).
9. N. S. Sariciftci and A. J. Heeger, U.S. Patent 5,331,183 (1994); U.S. Patent 5,454,880 (1995).
10. G. Yu and A. J. Heeger, *J. Appl. Phys.* **78**, 4510 (1995).
11. J. J. M. Halls *et al.*, *Nature* **376**, 498 (1995).
12. Electrical measurements were performed with a

Keithley 236 Source-Measure Unit. The excitation source was a tungsten-halogen lamp with a band-pass filter (centered at 430 nm, with a bandwidth of 100 nm). The maximum optical power at the sample was ~20 mW/cm².

13. F. Wudl, P.-M. Allemand, G. Srdanov, Z. Ni, D. McBranch, in *Materials for Nonlinear Optics Chemical Perspectives*, S. R. Marder, J. E. Sohn, G. D. Stucky, Eds. (American Chemical Society, Washington, DC, 1991), pp. 683-686.
14. J. C. Hummelen, B. W. Knight, F. Lepec, F. Wudl, *J. Org. Chem.* **60**, 532 (1995).
15. I. D. Parker, *J. Appl. Phys.* **75**, 1656 (1994).
16. I. H. Campbell, D. L. Smith, J. P. Ferraris, *Appl. Phys. Lett.* **66**, 3030 (1995).
17. η_e was calculated from the relation $\eta_e = FF I_{sc} V_{oc} / P_{in}$ using the following definition of filling factor:

$$FF = \int_0^{V_{oc}} IdV / I_{sc} V_{oc}$$

[see (8)]. In engineering applications, another definition of FF is sometimes used $FF = I_m V_m / I_{sc} V_{oc}$ where I_m and V_m are current and voltage for maximum power output. The FF and the η_e following this definition are approximately half of the values shown in the text.

18. The authors are grateful to N. S. Sariciftci and C. H. Lee for many valuable discussions. Supported by the Department of Energy under a grant from the Advanced Energy Projects Program (DOE-FG03-93ER12138).

20 June 1995; accepted 25 October 1995